16th World Conference on Earthquake Engineering, 16WCEE 2017
Santiago Chile, January 9th to 13th 2017
Paper N° 4575
Registration Code: S-A1466196534

# Reversed Cyclic Tests of Cylindrical Concrete Containment Structures

Hsuan-Chih Yang [1], Chiun-Lin Wu [2], Thomas T.C. Hsu [3]

[1] Associate Research Fellow, National Center for Research on Earthquake Engineering, Taipei, Taiwan hcyang@ncree.narl.org.tw
[2] Research Fellow, National Center for Research on Earthquake Engineering, Taipei, Taiwan
[3] Professor, Department of Civil and Environmental Engineering, University of Houston, Houston TX, USA

## Abstract

Nuclear containment structure is one of the most important infrastructure systems ensuring the safety of a nuclear power plant. In this paper, the structural behavior of the cylindrical vessels were investigated using two 1/13-scaled nuclear containment specimens subjected to reversed cyclic loadings. The presentation will first describe the test program and the test specimens, including the dimensions, the reinforcement detailing, the test setup, and the loading method. Second, the experimental results of the specimens are discussed including the cracking patterns, the total load versus displacement curves and the failure modes. Third, the test results were compared to the analytical results predicted at University of Houston using a 3-D finite element program with the CSMM-based shell elements. The predicted results agree very well with the experimental data.

*Keywords: RC containment vessel, cyclic test, scaled model*

# 1. Introduction

A reinforced concrete containment vessel (RCCV) is considered to be one of the key contributors to a NPP (Nuclear Power Plant) system's Defense in Depth (DID) strategy. The National Center of Research on Earthquake Engineering (NCREE) and the University of Houston, USA, cooperated to design and to build two RCCV cylindrical shell specimens in order to investigate their mechanical behavior and failure mechanism. These cylindrical shell specimens are 1/13 scaled models of a prototype RCCV used in an ABWR (Advanced Boiling Water Reactor) NPP. The ABWR is a Generation III boiling water reactor currently offered by GE Hitachi Nuclear Energy (GEH) and Toshiba. These reactors were first built in Japan, and one is under construction in Taiwan.

The containment is typically an airtight structure enclosing the reactor normally sealed off from the outside atmosphere. The design and thickness of the containment and the missile shield are governed by federal regulations. The integrity research of containments proposed by Sandia National Laboratories were incorporated in the design of BWR and PWR power plants. A lots of test projects were designed by using muti-scale, multi-process testing, large-scale validation experiments and phenomenological modeling in chemical, structural and thermal of contaiment strutures to identify the characteristics of containment. Three-dimensional finite element dynamic analyses were performed to evaluate the general capabilities of concrete-structures analytical methods and validation of the methods and interpretation of the test results (NUREG/CR-6906; NUREG/CR-6639).

A series of studies have focused on the structural behavior of RCCVs by using the cyclic tests and shaking table tests in Japan. The scaled RCCV structure with full boundary conditions, including top slab, tunnel, and fuel-pool girders, were constructed to confirm the trial-designed RCCV to be safe and reliable at a design-load level. The finite element analysis with 3-D solid elements was used to estimate the deformation, failure load and nonlinear behavior of RCCVs (H. Saito etc., 1991; H. Saito etc., 1993). The ultimate strength and seismic margin by an excitation that led to the model's collapse were determined and verified. The seismic characteristics of RCCVs and their structural behavior were indentified. (T. Hirama etc., 2005).

From a structural point of view, a nuclear containment can be visualized as assemblies of many elements. This concept facilitates the analysis of the complex structure when the finite element analysis is used, accompanied by the rational constitutive laws of materials. The key to rational analysis of the structure is to understand fully the behavior of one element isolated from the structure. Once a rational model is developed to predict the behavior of one element, this rational model can be incorporated into a finite element analysis program, such as OpenSees (2013), to predict the behavior of the whole structure under different kinds of loading.

A finite element method was developed at the University of Houston (UH) based on OpenSees. The UH method utilized wall elements based on the Cyclic Softened Membrane Model (CSMM) (Mansour & Hsu, 2005; Hsu & Mo, 2010). The constitutive laws CSMM was developed at UH using the Universal Panel Tester (Hsu, Belarbi, and Xiaobo, 1995). This finite element method was recently extended to include CSMM-based shell elements (Xiang, Mo, and Hsu, 2012) and (Luu, 2016), and is called Program SCS-3D. Program SCS-3D is capable of predicting the reversed cyclic behavior of cylindrical reinforced concrete containment structures.

# 2. Experimental program

## 2.1 Specimen Design

The size of test specimens should be as close as possible to the structure to properly represent its true behavior. Based on the current capacity of testing equipment at the NCREE laboratory in Taipei, Taiwan, the experimental specimen of 1/13-scaled nuclear containment vessel was designed to investigate the behavior of a nuclear containment vessel isolated from a nuclear plant and subjected to the gravity and earthquake loads. This section describes the test specimens, material properties, construction process, test setup, instrumentation, and loading protocol.

The specimen was designed based on the prototype of an Advanced Boiling Water Reactor (ABWR) nuclear containment structure, as shown in Figure 1(a). The real-size containment has a height of 29.5 m, a radius of 15.5 m (center-line dimension), and a thick wall of 2.0 m, as shown in Figure 1(b). To simulate the loads and keep the boundary conditions of the specimens as close to the real nuclear containment structure as possible, a computer-controlled static testing system with multiple displacement and force control modes was used. A control scheme was developed to apply the lateral load following a displacement history while maintaining a constant axial load and preventing rotation at the top of the specimen.

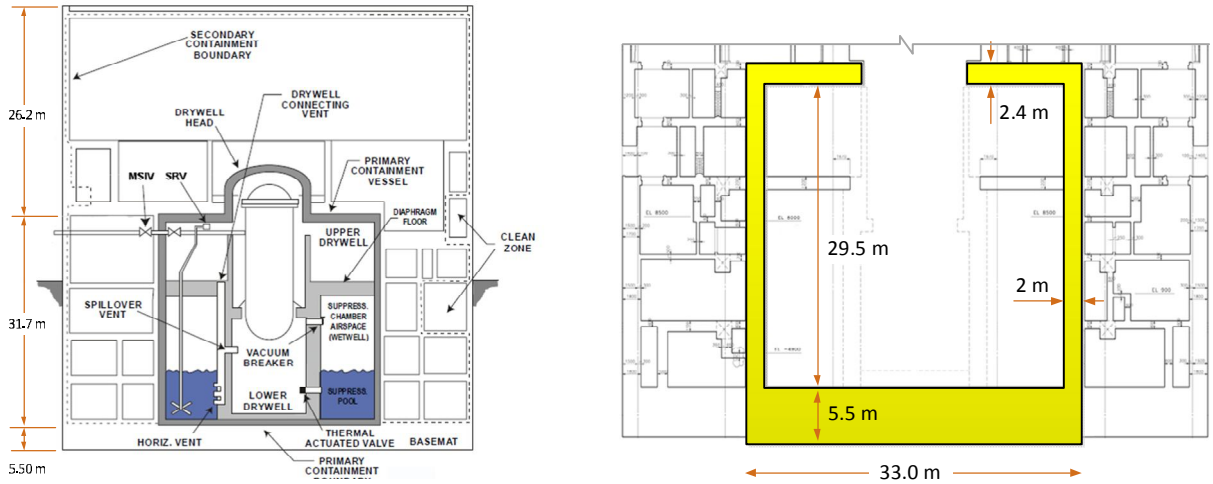


(a) Elevation view (b) Prototype of test specimen

Figure 1 ABWR Nuclear Power Plant

The experimental program included the construction and testing of two nuclear containment specimens under axial and lateral loading. The specimens had similar amount of reinforcement ratio compared to the real structure. The test specimens, which were connected to nearly rigid top and bottom slabs, were tested in double curvature. The sizes of the test specimens are shown in Figure 2. Due to their size and capacity, similar types of tests have not been reported in the literature; therefore, the tests are unique.

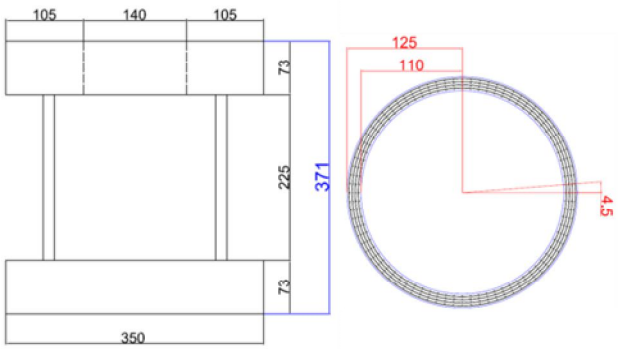


Figure 2 Dimensions of the RCCV Test Specimens

## 2.2 Specimen Description

Each specimen included three parts: the main containment, top slab, and bottom slab. The bottom slab simulated the rigid foundation while the top slab simulated the rigid floor system. These slabs were designed conservatively to avoid significant deformation occurring in the slabs so that the nonlinearity took place only in

the containment during the tests. Rotations of the top and base slabs in the vertical plane were prevented during the test to ensure the containments had double-curvature behavior during the tests.

The reinforcement arrangement in the specimens is illustrated in Figure 3. Four layers of vertical and circumferential reinforcements were along the thickness of the containments. The #3 (diameter of 9.5 mm) and #2 (diameter of 6.4 mm) deformed steel bars were adopted in the test containment for vertical and circumferential reinforcements, respectively, and the steel bars in the top and bottom slabs were #5 (diameter of 15.8 mm). The reinforcements were uniformly distributed around the perimeter and along the height of the main containment of Specimen No. 1 with the same spacing. The percentage of the reinforcement ratio in the containment of Specimen No. 1 was 2% in both the vertical and circumferential directions. The vertical bars in the containments were continuous without lap splices. The clear concrete cover over the vertical bars was 17 mm. The circumferential bars were closed using welding lap splices with a length of 30 db, where db was the bar diameter. The anchorage length of the vertical bars of the containments inside the top and bottom slabs was greater than the development length calculated using ACI 318-11. The joint connector nuts were provided at the end of the vertical bars to further enhance the anchorage capacity during the tests.

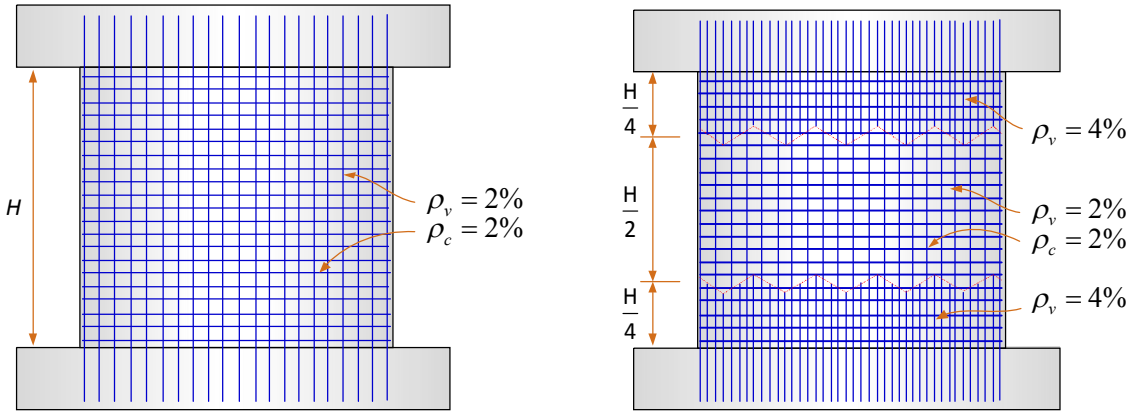


(a) Specimen No. 1 (b) Specimen No. 2

Figure 3 Reinforcement details of the RCCV specimens

Table 1 Dimensions and Material Properties of RCCV Specimens

| Specimen No. | $f'_C$ (MPa) | $D$ (mm) | $H$ (mm) | $t$ (mm) | Vertical Reinforcement | | | Circumferential Reinforcement | | |
|---|---|---|---|---|---|---|---|---|---|---|
| | | | | | $d_b$ (mm) | $f_y$ (MPa) | $\rho_v$ (%) | $d_b$ (mm) | $f_y$ (MPa) | $\rho_c$ (%) |
| RCCV#1 | 37 | 2350 | 2250 | 150 | 9.5 | 379 | 2 | 6.4 | 376 | 2 |
| RCCV#2 | 43.5 | 2350 | 2250 | 150 | 9.5 | 379 | 2 or 4 | 6.4 | 376 | 2 |

Note : $f'_c$ = Compressive strength of concrete; $D$ = Diameter; $H$ = Net height;
$t$ = Thickness; $f_y$ = Yielding strength of steel; $d_b$ = Diameter of steel bar;
$\rho_v$ = Steel ratio in the vertical direction; $\rho_c$ = Steel ratio in circumferential direction

The reinforcement details of Specimen No. 2 is almost identical to Specimen No. 1 except that more vertical reinforcements (dowel bars) were added to each end of the containment to enhance its shear sliding capacity, resulting in the vertical reinforcement ratio of 4% in each of these two ends, as shown in Figure 3(b). The cut-off points of the additional vertical reinforcement were arranged in a jagged manner to prevent cracking within the

cut-off regions. The center line of the zigzag curve was at a quarter of the containment height. The details of dimensions and material properties of the specimens are summarized in Table 1.

## 2.3 Material

A local concrete company supplied the ready-mixed concrete for the test specimens. Similar concrete mixtures were used for both specimens. Because of the high amount of reinforcements placed in a slender wall of the containments, using traditional concrete would have caused difficulty in the concrete consolidation in such congested reinforced specimens. As a result, self-consolidating concrete (SCC) was used in the specimens. Self-consolidating concrete, also referred to as self-compacting concrete, has substantial commercial benefits because of the ease of placement in complex forms with congested reinforcements. The filling ability and flowability of the SCC mixture were tested using the slump flow test. The slump flow is the mean diameter of the horizontal spread of the concrete mass, after lifting the slump cone. The slump flow diameters of the SCC mixture were 75 cm and 71 cm for RCCV#1 and RCCV#2, respectively.

## 2.4 Instrumentations

The overall system instrumentation used can be categorized into internal and external instrumentation systems. The internal instrumentation included the strain gauges used to measure the reinforcement strains at selected positions. The external instrumentation encompassed load cells, Linear Voltage Displacement Transducers (LVDTs), dial gauges, and the Northern Digital Inc. motion capture system equipped with four Optotrak Certus HD Position Sensors.

## 2.5 Test Setup

The test specimens were subjected to horizontal loading up to their maximum capacity with a set of specially built steel loading frames at the National Center for Research on Earthquake Engineering, Taiwan, as shown in Figure 4. The test setup was used to simulate gravity and the lateral and vertical earthquake loads. Figure 4 shows the overview of the test setup with various components in details, including the horizontal actuators, vertical actuators, steel loading frame systems, and the specimen and data acquisition systems.

(a) Specimen RCCV 1 (b) Specimen RCCV 2

Figure 4 Test Set-up of the RCCV specimens

The specimens were loaded axially using four 980-kN capacity vertical hydraulic actuator. Pin connections were used at the end of the vertical actuators to minimize moment when transferred to the L-shaped steel loading frame. The simulated lateral earthquake load was applied by eight 980-kN-capacity horizontal actuators under displacement control. The horizontal actuators were bolted to a rigid concrete reaction wall and the L-shape loading frame such that the center of the loading axis passed through the specimen's mid-height. Additional supporting steel frames bolted to the strong floor were placed on the north and south sides of the specimen to prevent the horizontal out-of-plane displacement.

During the tests, the containment specimens were subjected to constant vertical axial loads and horizontal reversed-cyclic load until failure. Both the prescribed displacement and forces controlled the four vertical actuators. A prescribed horizontal displacement history controlled the eight horizontal actuators. A control code in the computer-control testing system controlled the operation of the vertical and the horizontal actuators.

### 2.6 Loading Protocol

The first step of the loading protocol program was to apply an axial load that would remain constant during the course of the test. The total initial vertical load equaled 1.6% of the axial concrete capacity ($f_c'A_g$) of each specimen, where $f_c'$ is compressive strength of concrete and $A_g$ is nominal area of the specimen. The axial concrete capacity was dependent on the compressive strength of the concrete ($f_c'$); consequently, the total initial vertical load varied for each specimen.

After the axial load was applied, a reversed-cyclic load was added by eight 980-kN-capacity horizontal actuators under displacement control. First, the test specimens were subjected to several cycles of small displacements for warming up, in which the specimen behaved elastically. Then, inelastic tests were performed by using the loading history shown in Figure 5.

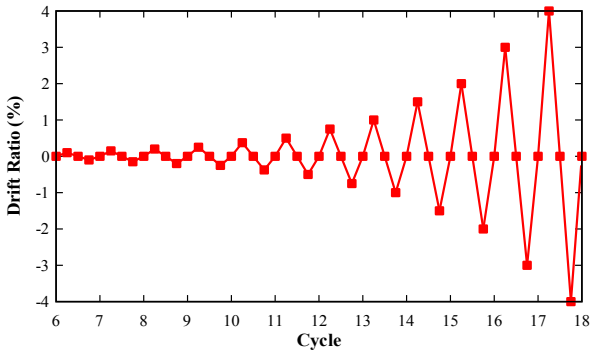


Figure 5 Horizontal displacement control scheme (Inelastic test)

## 3. Experiment results

### 3.1 Load-Displacement Characteristic

The horizontal load versus horizontal displacement relationships of the test specimens are shown as dashed curves in Figure 6. These curves illustrate the load resisting mechanism of the nuclear containment vessels. Five critical points are noted in each curve, i.e. the first cracking of concrete, the first yieldings of vertical and circumferential steel bars, and the peak loads. The slope of the envelope curve often decreased when the stiffness of the specimen was reduced significantly after cracking. The cracking loads of Specimen No. 1 and Specimen No. 2 were determined to be 1900 kN and 1880 kN, respectively.

By observing the strain data of all the steel bars at each step of loading, it is shown that both the vertical and circumferential steel bars of Specimen No. 1 yielded during the tests, and the yielding points of the steel bars were close to each other. In the positive loading direction, the vertical steel bars yielded first at the load of 3706 kN and the displacement of 7.84 mm; the circumferential steel bars yielded later at the load of 4234 kN and the displacement of 9.9 mm. Similarly, in case of Specimen No. 2, both the vertical and circumferential steel bars yielded during the test, and the circumferential steel bars reached yield before the vertical steel bars in both the positive and negative loading direction. In the positive loading direction, the circumferential steel bars yielded at the load of 3363 kN and the displacement of 7.04 mm; the vertical steel bars yielded at the load of 3702 kN and the displacement of 8.1 mm.

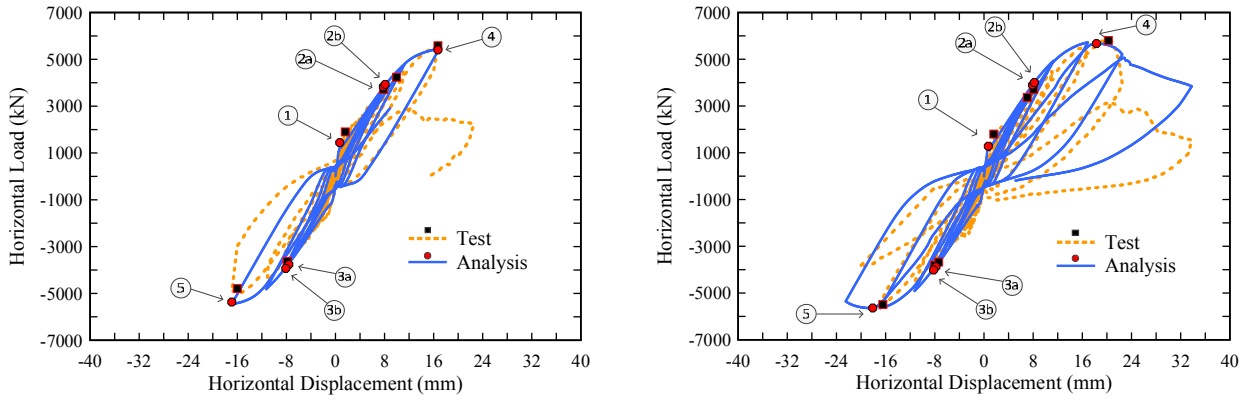


(a) Specimen No. 1 (b) Specimen No. 2

Figure 6 Comparison of experimental and analytical horizontal load versus displacement curves

The recorded peak loads of Specimen No. 1 were 5580 kN and 4794 kN in the positive and negative loading directions, respectively. The displacements corresponding to the peak loads were 16.7 mm and 16.0 mm in the positive and negative loading directions, respectively. The recorded peak loads of Specimen No. 2 were 5805 kN and 5487 kN in the positive and negative loading directions, respectively. The displacements corresponding to the peak loads were 20.2 mm and 16.5 mm in the positive and negative loading directions, respectively. It can be seen that the peak loads of Specimen No.2 were slightly higher than the peak loads of Specimen No.1 in both loading directions. In both specimens, the lateral strength dropped significantly after the peak load.

As observed from the load versus displacement curves, because the steel bars yielded before the loads reached the peak, it can be concluded that the specimens had ductile behavior. The ductility coefficients were calculated as the ratio of displacement at the peak load divided by the first yielding displacement of the specimens. In the positive loading direction, the ductility coefficients of Specimen No. 1 and Specimen No. 2 are 2.13 and 2.87, respectively. In the negative loading direction, the ductility coefficients of Specimen No. 1 and Specimen No. 2 are 2.04 and 2.23, respectively.

## 3.2 Failure Modes

The two test specimens were almost identical; however, the failure modes of the two specimens were very different. Specimen No. 1 failed due to sliding shear that happened at the top of the specimen, as shown in Figure 7(a). The peak load of Specimen No. 1 might have been higher if the sliding shear had not occurred. The sliding shear cracks started to occur on the top of the specimen at a drift of 0.5% and became larger when the load increased. Before the sliding shear failure, no critical damage of the concrete and reinforcement was observed in the specimens. Learning from the failure of Specimen No. 1, additional vertical steel bars, called dowel bars, were added on the top and bottom of Specimen No. 2 to prevent the sliding shear failure. The method was successful because no sliding shear failure occurred and the sliding shear cracks on the top of the specimen were eliminated. As a result, the specimen No. 2 failed when the concrete crushed in the mid-height region due to web shear failure, and the specimen reached a higher peak load and deformation.

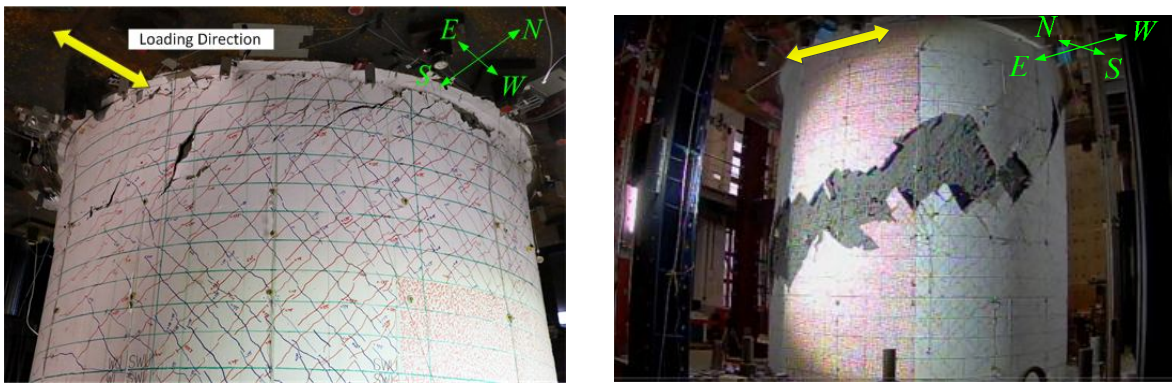


(a) Specimen No. 1: Sliding shear (b) Specimen No. 2: Web shear

Figure 7 Failure modes of the RCCV specimens

## 4. Analytical Model

### 4.1 Finite Element Mesh

In this section, the tested RCCV specimens were analyzed by using the CSMM-based shell element to validate the capacity of the element in predicting the behavior of shell-type structures such as nuclear containment vessel under reversed cyclic loading. The specimens were modeled using the finite element mesh illustrated in Figure 8(b). For each specimen, the cylindrical wall of the vessel was defined by 40 CSMMShellS8 elements. Ten layers of concrete and two layers of steel were assigned for each element using the CSMMLayer material module (Figure 8(a)). Mesh sensitivity analyses, which were conducted before the analysis to ensure that the predicted results were not sensitive to the finite element size under the current mesh used. The steel layers were defined at the exact locations of the steel within the cross section of the specimen. In Specimen No. 1, all shell elements were assigned with 2% of reinforcement in both vertical and circumferential directions. The percentage of steel used in shell elements of Specimen No. 2 was almost identical to Specimen No. 1, except the shell elements located within the region of one-fourth of the net height at the top and bottom of the specimen were assigned with 4% of vertical reinforcement.

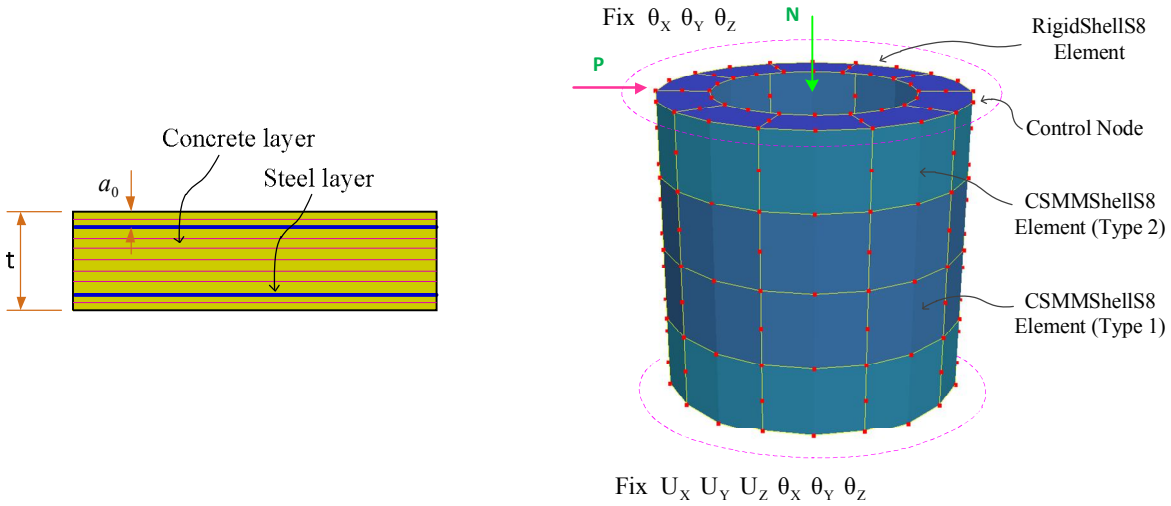


(a) Finite element mesh along the thickness (b) Finite element mesh of Specimen No. 2

Figure 8 Finite element modeling of Specimen No. 2

The top slab of each RCCV specimen was defined as a rigid body by using ten CSMMShellS8 elements with high stiffness. For the boundary conditions, all nodes at the bottom of the model were constrained to not allow any translations or rotations. Equal horizontal and vertical loads were applied at all nodes along the perimeter at the height level of the specimen based on the assumption that the loads were uniformly distributed. The axial loads acting on the cap were applied with the direction and magnitude of the loads remaining constant in the analysis. The horizontal loads were changed according to the displacement control scheme.

### 4.2 Analytical Algorithm

The analysis was performed by a predetermined force control and displacement control schemes. Axial loads were kept constant and reversed cyclic horizontal loads are applied by the predetermined displacement control on the drift displacement. The common displacement increment used in the analysis was 0.5 mm. Convergence was obtained smoothly during the cyclic analysis. The KrylovNewton method was used as the solution algorithm. The nodal displacement and corresponding horizontal forces were recorded at each converged displacement step, and the stress and strain of the elements were also monitored. The results of the sensitivity analysis showed that using 40 elements with 2 layers was sufficient for finite element analysis of RCCV specimens.

## 5. Comparison of Analytical Results with Experimental Outcomes

The horizontal load versus the horizontal displacement relationships of the test specimens are also shown in Figure 5 as solid curves. Five critical points were indicated in each curve to compare the analytical results with the experimental data. The critical points corresponded to the first cracking of concrete, the first yielding of vertical and circumferential steel bars, and the peak loads in each specimen. The analytical cracking loads of Specimen No. 1 and Specimen No. 2 were 1443 kN and 1490 kN, respectively. The analytical cracking loads were slightly smaller than the cracking loads obtained from the tests.

The analytical model accurately predicted the yielding condition of steel bars, in which it showed that the vertical and the circumferential steel bars both yielded during the test and that the first yielding points of the vertical and circumferential steel bars were close to each other. In Specimen No. 1, the analytical model predicted that the vertical steel bars yielded first in both the positive and negative loading direction. In the positive loading direction, the first yielding load was 3829 kN at the yielding displacement of 7.8 mm, respectively. In the negative loading direction, the first yielding load was 3764 kN at the yielding displacement of 7.6 mm. In Specimen No. 2, the analytical model predicted that the circumferential steel bars yielded first in both the positive and negative loading direction. In the positive loading direction, the first yielding load was 3897 kN at the yielding displacement of 7.9 mm. The predicted yielding loads and yielding displacements of the tests specimens are shown to have good correlations with the experimental data.

For Specimen No. 1, the peak loads predicted were 5400 kN and 5367 kN in the positive and negative loading directions, respectively. The displacements corresponding to the peak loads were 16.7 mm and 16.9 mm in the positive and negative loading directions, respectively. For Specimen No. 2, the peak loads predicted were 5669 kN and 5640 kN in the positive and negative loading directions, respectively. The displacements corresponding to the peak loads were 18.3 mm and 18.1 mm in the positive and negative loading directions, respectively. The predicted peak loads and peak displacements of the tests specimens are shown to have good correlations with the experimental data.

The analytical horizontal force versus displacement relationships of the test specimens were compared with the experimental results. The experimental result and the analytical result are illustrated by a dashed curve and a solid curve, respectively. The analytical result provided a good correlation with the experimental data. Although the predicted initial stiffness was higher compared to the experimental stiffness, the analytical model accurately predicted behaviors in the both positive and negative directions, including the primary backbone curve, the initial stiffness, the yield points, and the peak strength. Furthermore, the unloading path and pinching behavior were well simulated.

## 6. Copyrights



## 7. References

1. NUREG/CR-6906, SAND2006-2274P, "Containment Integrity Research at Sandia National Laboratories An Overview ", July 2006
2. NUREG/CR-6639, SAND99-1464, ANA-98-0252, "Seismic Analysis of a Prestressed Concrete Containment Vessel Model", March 1999
3. H. Saito, Y. Muramatsu, H. Furukawa, S. Tsurumaki, N. Tanaka and T. Kei, "Experimental study on RCCV of ABWR plant", Nuclear Engineering and Design 130, 1991, pp179-202
4. H. Saito, Y. Muramatsu, H. Furukawa, T. Hasegawa and A. Mutoh, "Post-test analysis of a 1:10-scale top slab model of ABWR/RCCV subjected to internal pressure", Nuclear Engineering and Design 145, 1993, pp339-353
5. T. Hirama, M. Goto, K. Shiba, T. Kobayashi, R. Tanaka, S. Tsurumaki, K. Takiguchi, H. Akiyama, " Seismic proof test of a reinforced concrete containment vessel (RCCV) Part 2: Results of shaking table tests", Nuclear Engineering and Design 235, 2005, pp1349–1371
6. Hsu, T. T. C., Belarbi, A., & Xiaobo, P. (1995). A Universal Panel Tester. Journal of testing and evaluation, 23(1), 41-49.
7. Luu, C. H. (2016). Development of CSMM-Based Shell Element for Reinforced Concrete Structures. (PhD Dissertation), University of Houston.
8. Hsu, T. T. C., & Mo, Y. L. (2010). Unified Theory of Concrete Structures: John Wiley & Sons.
9. Mansour, M., & Hsu, T. T. C. (2005). Behavior of Reinforced Concrete Elements under Cyclic Shear: Part 1 – Experiments. Journal of Structural Engineering, ASCE, 131(1), 44-53.
10. OpenSees. (2013). Annual Workshop on Open System for Earthquake Engineering Simulation. Paper presented at the Pacific Earthquake Engineering Research Center, UC Berkeley.
11. Xiang, H. J., Mo, Y. L., & Hsu, T. T. C. (2012). Seismic Simulation of RC Wall-type Structures using Softened Shell Model. 建筑结构学报 (Journal of Building Structures), v3, Beijing. (in Chinese).